OPTOELECTRONICS AND ADVANCED MATERIALS – RAPID COMMUNICATIONS Vol. 1, No. 4, April 2007, p. 145 - 148

Nonlinear least squares algorithm with embedded Kalman filter for Bragg wavelength detection in fiber Bragg grating sensors

YU TANG*, YUN CHUNG CHU, CHI CHIU CHAN[a], JIAN SUN[a]
School of Electronic Engineering, Nanyang Technological University, Singapore 639798
[a]School of Chemical and Biological Engineering, Nanyang Technological University, Singapore 637457

In a fiber Bragg grating (FBG) sensing system, the accuracy of Bragg wavelength detection is much affected by the presence of unwanted interferometric signal in the system. In this paper, a nonlinear least-square (NLS) algorithm with an embedded Kalman filter is used to remove this unwanted signal to enhance the measurement accuracy. This hybrid approach avoids the disadvantage of a pure NLS estimation, which is rather model sensitive, and the disadvantage of an extended Kalman filter, which might fail to converge. Computer simulations and experimental results are provided to demonstrate the effectiveness of this proposed method. Improvements of the accuracy in Bragg wavelength detection are observed.

(Received January 25, 2007; accepted March 14, 2007)

Keywords: Fiber Bragg grating, Nonlinear least squares, Kalman filter

1. Introduction

To accurately measure strain or thermal variations using fiber Bragg grating (FBG) sensors, small drifts of the Bragg wavelength should be detected [1-3]. Two kinds of schemes have been proposed. The first kind applies a broadband source and various spectral analyzing techniques such as edge filters, scanning Fabry-Pérot filters, acousto-optic tunable filters and Mach-Zehnder interferometers [4], [5]. However, the broadband source provides a low signal power to the receiver, resulting in a low signal-to-noise ratio (SNR). The second scheme makes use of a tunable laser source with a broadband detector [6].

This provides a high signal power to enhance the SNR, but implies an unwanted interferometric signal, which contaminates the FBG spectrum and is not easy to remove. Previously, digital low-pass filters [7] were applied but the improvement was limited because the free-spectral range (FSR) of the unwanted interferometric signal was comparable with or larger than the full-width at half-maximum (FWHM) of the FBG [8]. In this paper, an alternative method is proposed. The new method basically treats the Bragg wavelength detection as a parameter estimation problem instead of a filtering problem. The advantage is that it can better utilize the mathematical model of the spectrum, presented in Section 2, to give potentially better results, although it can also be argued that such an approach is model sensitive. Therefore, the proposed method combines nonlinear least-square (NLS) estimation with Kalman smoothing. As will be seen in Sections 3 and 4, this hybrid approach avoids the disadvantage of a pure NLS estimation, which is rather model sensitive, and the disadvantage of an extended Kalman filter, which might fail to converge. Computer simulations in Section 4 and experimental results in Section 5 show that the Bragg wavelength detection accuracy is greatly enhanced. The experimental results also confirm the applicability of the proposed method to a real sensing system, despite that the mathematical model in Section 2 is not always perfect.

2. Spectrum model

The schematic diagram of the FBG sensing system is shown in Fig. 1. The narrow-band laser light is delivered from a tunable light source and passes to an FBG sensing system via a 3dB 2×2 coupler.

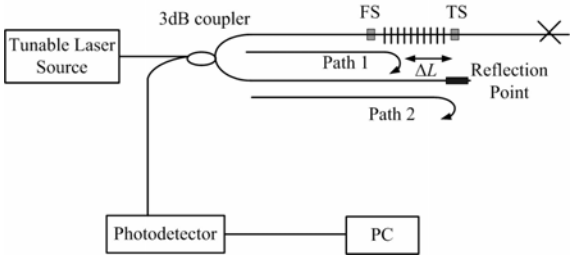

Fig. 1. Schematic diagram of the setup (FS: fixed stage, TS: translation stage, PC: personal computer).

Half of the light intensity passes through one arm of the coupler and reaches the FBG. Another half of the light intensity passes to the other arm of the same coupler. The light of the Bragg wavelength is reflected by the FBG via the same coupler again and is detected by a broadband photodetector (Path 1). On the other hand, some reflected light is detected by the photodetector from a reflection point of the other arm of the same coupler (Path 2). This reflected light will interfere with the light reflected from the FBG and cause an unwanted interferometric signal. As a result, the Bragg wavelength will be contaminated by

this unwanted reflected signal, which degrades the Bragg wavelength detection accuracy.

The spectrum at the photodetector can be written as [7]:

$$I_{meas}(\lambda) = I_s(\lambda) + I_{sn}(\lambda) + I_{wn}(\lambda) \quad (1)$$

where λ is the wavelength. $I_s(\lambda)$ is the spectrum in ideal conditions,

$$I_s(\lambda) = I_0/4 \cdot R(\lambda - \lambda_B) \quad (2)$$

and $R(\lambda - \lambda_B)$ represents the reflective spectrum of the FBG, centered at the Bragg wavelength λ_B. I_0 is the intensity of the tunable laser source, which may be regarded as constant within a tuning range. $R(\bullet)$ is typically (but not necessarily) modeled as a Gaussian function with a peak reflectivity of R_0 and a spectral full-width at half-maximum (FWHM) of $\Delta\lambda_B$:

$$R(\lambda - \lambda_B) = R_0 \exp(-4\ln 2(\lambda - \lambda_B)^2/(\Delta\lambda_B{}^2)) \quad (3)$$

$I_{sn}(\lambda)$ in Eq. (1) represents the unwanted interferometric signal, modelled as

$$I_{sn}(\lambda) = \sqrt{I_s(\lambda)} \cdot \alpha\sqrt{I_0}\cos(2\pi n\Delta L/\lambda + \phi) + \alpha^2 I_0/4 \quad (4)$$

where α^2 is the intensity reflectivity of the reflection point, n is the reflexive index of the optical fiber, ΔL is the path difference between the signal wave and the reflected wave from the reflection point, and ϕ is a random phase factor caused by the environmental disturbances. Finally, $I_{wn}(\lambda)$ in Eq. (1) represents a random noise from the tunable laser source. Under proper assumptions, $I_{wn}(\lambda)$ may be modelled as a Gaussian-white noise with mean σ^2 and variance $2\sigma^4/N$, with $N > 50$. (If the noise level were higher, a different noise model could be used so that $I_{meas}(\lambda)$ would be non-negative).

Fig. 2 shows a typical example of I_{meas} in the computer simulations, where the Gaussian model Eq. (3) of the FBG is assumed with λ_B = 1550 nm, and N for the random noise $I_{wn}(\lambda)$ is chosen as 200. (Details of other settings can be found in Section III). Note that due to the unwanted interferometric signal $I_{sn}(\lambda)$, the detection of the Bragg wavelength λ_B becomes a challenging task. When $n\Delta L$ is relatively large, conventional filtering techniques are effective in removing I_{sn} since the FSR of I_{sn} is much smaller than the FWHM of I_s. However, they fail when $n\Delta L$ is small. As a mathematical model of the spectrum is available, this paper treats the detection of λ_B as a parameter estimation problem rather than a filtering problem.

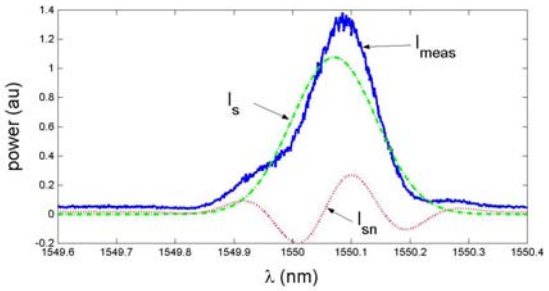

Fig. 2. Typical spectrums I_{meas}, I_s, I_{sn} in the computer simulations.

3. Nonlinear least-square estimation

Although the computer simulations will adopt a Gaussian model of $R(\bullet)$, it might be inaccurate for experimental data and therefore will be dropped in the theoretical development below. Instead, $R(\bullet)/R_0$ is assumed general but available, i.e., the shape of $R(\lambda - \lambda_B)$ is provided but not its magnitude R_0 or its location λ_B. It will be obvious from the development that the proposed method works with an arbitrary scaling of $R(\bullet)/R_0$. Hence, for the simplicity of notation, R_0 is assumed 1 and $R(\bullet)$ is assumed given.

Table 1. Ranges of parameter values in the computer simulations.

	minimum	maximum
$\ln(I_0/4 \cdot R_0)$	-0.1	0.1
λ_B	1550-0.1	1550+0.1
$\log(\Delta\lambda_B)$	0.1	0.4
$\ln(2\alpha/\sqrt{R_0})$	-2	-1
ϕ	$-\pi$	π
$\log(n\Delta L)$	$\log(2 \times 1550^2)$	$\log(12.5 \times 1550^2)$
$\ln(1 + 4\sigma^2/(\alpha^2 I_0))$	0.8	1.2

The spectrum model introduced in Section II has six parameters: I_0, λ_B, α, ϕ, $n\Delta L$ and σ^2, which may not be known but can be estimated from the measured data. Nonlinear least square (NLS) is a well-established technique in parameter estimation [9] and can be applied directly to estimate the six unknown parameters from the measured spectrum $I_{meas}(\lambda)$. However, this is not the most effective way as the larger the number of parameters,

the more time the NLS algorithm consumes and also the higher the chance that it gets trapped into a local minimum. Instead, this paper formulates the problem at hand as an NLS problem of 2 variables, within which a linear least-square problem of 4 variables will be solved. To this end, Eq. (1) is rewritten as

$$I_{meas}(\lambda) = x_1 R(\lambda - \lambda_B) + x_2 \sqrt{R(\lambda-\lambda_B)}\cos(2\pi n\Delta L/\lambda) - x_3 \sqrt{R(\lambda-\lambda_B)}\sin(2\pi n\Delta L/\lambda) + x_4 + v(\lambda) \quad (5)$$

where $x_1 = I_0/4$, $x_2 = \alpha I_0/2\cdot\cos\phi$, $x_3 = \alpha I_0/2\cdot\sin\phi$, $x_4 = \alpha^2 I_0/4 + \sigma^2$ and $v(\lambda)$ is a zero-mean Gaussian-white noise. Hence, when λ_B and $n\Delta L$ are fixed, x_i can be estimated from the measured data I_{meas} as a linear least-square (LLS) problem. This reduces the original NLS problem into a problem of 2 variables only, namely λ_B and $n\Delta L$.

To verify the effectiveness of this NLS-LLS approach, 4,000 random spectra similar to the one in Fig. 2 were used in the computer simulations, with the actual parameter values randomly generated and uniformly distributed in the ranges shown in Table 1. The measured spectrum I_{meas} was sampled at an 1 pm step. For comparison, a conventional low-pass finite impulse response (FIR) filter followed by peak-detection was also used. Fig. 3 summarizes the cumulative distribution functions of the estimation error in λ_B over the 4,000 random spectrums. FIR has a 90% confidence interval of [-33.5, 34.4] pm while NLS-LLS has a 90% confidence interval of [-0.8112, 0.9007] pm. The detection accuracy has been improved by more than 30 times.

4. Kalman smoothing

Despite its success in the computer simulations, NLS-LLS does not work equally well for experimental data. It is because NLS estimation is relatively model sensitive. The spectrum model in Section 2 is good but by no means perfect. To overcome this problem, a Kalman filter (KF) is proposed to replace the LLS engine inside the NLS estimation. The underlying idea is to relax the assumption of x_i being a constant to a Wiener random process, allowing x_i to be slowly varying over λ. This relaxation can effectively reduce the sensitivity of the algorithm to the spectrum model.

Let h denote the sampling step of $I_{meas}(\lambda)$. A state-space model for $x = (x_1, x_2, x_3, x_4)$ can be constructed:

$$x(\lambda + h) = x(\lambda) + u(\lambda) \quad (6)$$

$$I_{meas}(\lambda) = C(\lambda)x(\lambda) + v(\lambda) \quad (7)$$

$$C(\lambda) = \begin{bmatrix} R(\lambda-\lambda_B) \\ \sqrt{R(\lambda-\lambda_B)}\cos(2\pi n\Delta L/\lambda) \\ -\sqrt{R(\lambda-\lambda_B)}\sin(2\pi n\Delta L/\lambda) \\ 1 \end{bmatrix}^T \quad (8)$$

where the "system noise" u and the "measurement noise" v are Gaussian-white. If the variance of u is zero, x is constant over λ as in Section 3. In general, by controlling the covariance matrices of u and v, various degrees of mismatch between the four terms in Eq. (5) and the experimental data I_{meas} can be considered, making this method very flexible when a Kalman filter is applied to estimate the unknown state-vector x.

It is actually possible to apply the idea of Kalman filtering to estimate all six unknown parameters of I_{meas}. However, this will lead to an extended Kalman filter. This paper proposes to replace only the LLS engine within the NLS estimation by a Kalman filter, which will result in a linear time (λ)-varying system with guaranteed properties of convergence. In the end, the estimation algorithm will have an outer NLS estimation with an inner Kalman filtering routine. This hybrid NLS-KF approach seems to show a big improvement over a pure Kalman filtering approach, analogous to the advantage observed in Section 3 when a combined NLS-LLS estimation was used instead of a pure NLS estimation.

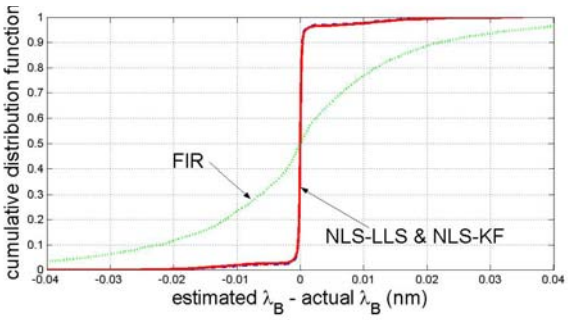

Fig. 3. Computer simulation results for λ_B.

Since the independent variable in the state-space model Eqs. (7)–(8) is the wavelength λ instead of time, casuality is not an issue and a Kalman smoother instead of a Kalman filter can be employed to give better results [10]. A Kalman smoother consists of both a forward filter and a backward filter, and the formulation adopted in this work is similar to that of Rauch-Tung-Striebel [11].

The NLS-KF approach was tested with the same 4,000 random spectrums from Section 3. The cumulative distribution function of the estimation error in λ_B is also summarized in Fig. 3, but the curve is hardly distinguishable from the one for NLS-LLS. The 90% confidence interval is actually [-0.7120, 0.7357]pm, which is about 15% narrower than that of NLS-LLS. This was not expected, since the spectrum model in the computer

simulations was exact, unlike the experiments in Section 5 below. Further examinations of the simulation results revealed that NLS-KF performed much better than NLS-LLS in estimating $n\Delta L$, the other unknown parameter of the problem. As shown in Fig. 4, NLS-LLS would underestimate $n\Delta L$ more easily, suggesting that it get trapped at a local minimum, while NLS-KF would not. This might indirectly improve the estimate of λ_B by NLS-KF as a result.

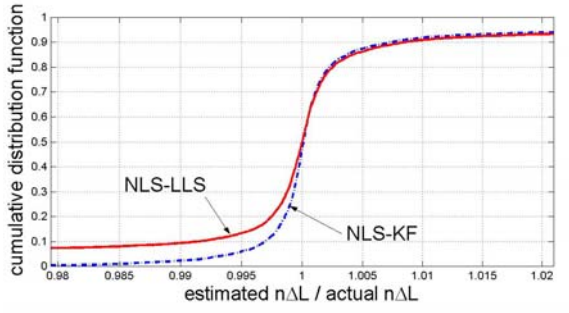

Fig. 4. Computer simulation results for $n\Delta L$.

5. Experimental results

Experiments were conducted using the setup shown in Fig. 1. The light from a tunable laser passed through a 3dB coupler and divided equally into two arms with one of them connected to an FBG sensor. The FBG was mounted on a fixed stage (FS) and a translation stage (TS) for the purpose of applying strain to change the Bragg wavelength λ_B. The reflected light from the FBG returned through the same coupler and was detected by a photodetector. The tuning step and range of the wavelength from the tunable laser were set as 1pm and 1nm, respectively. The signal from the photodetector was synchronously recorded by a personal computer (PC). Fig. 5 shows a typical measured spectrum I_{meas} in the experiments, together with the estimated I_s and I_{sn} using NLS-KF.

Table 2. Root-mean-square error in the estimation of λ_B (pm).

	1	2	3	4	5
FIR	5.5408	4.7854	5.4222	6.2530	4.2426
NLS-LLS	8.4669	5.4100	6.4496	7.7398	8.6305
NLS-KF	1.5681	1.0424	2.1458	1.8878	1.3971
	6	7	8	9	10
FIR	5.3944	6.8484	3.8210	2.7386	5.1672
NLS-LLS	6.9901	6.9841	3.9841	4.8732	7.8067
NLS-KF	2.7301	2.0494	2.1921	2.2648	4.6950

For each value of λ_B, a "good" spectrum without interferometric signal was first obtained to provide a reference spectrum $R(\bullet)$. Then 10 sets of I_{meas}, with different unwanted interferometric signal in different sets, were measured. The root-mean-square (RMS) error in the estimation of λ_B over these 10 sets was recorded. This procedure was repeated for 10 different values of λ_B and the 10 RMS values are summarized in Table 2. It was seen that FIR performed reasonably well because $n\Delta L$ was relatively large in the experimental data (> 1.5cm). Still, NLS-KF showed an improvement of about a factor of 2.

6. Conclusions

An NLS algorithm with an embedded Kalman filter has been presented in this paper for the removal of the unwanted interferometric signal from the contaminated FBG spectrums. Simulations and experimental results have confirmed a good accuracy of Bragg wavelength detection. Improvements over conventional filtering approaches have also been observed. Although the sensing system considered in this paper is relatively simple, the method can be easily adapted to other sensing systems as long as a suitable mathematical model exists. The combination of NLS estimation with Kalman filtering has effectively reduced the sensitivity to the model, thus increasing the potential of applying this method to a real sensing system, as confirmed by the experimental results presented in this paper.

References

[1] B. Culshaw, Smart Structures and Materials. Norwood: Artech House, 1996.
[2] E. Udd, Fiber Optic Smart Structures. New York: John Wiley & Sons, Inc., 1995.
[3] A. Othonos, K. Kalli, Fiber Bragg Gratings: Fundamentals and Applications in Telecommunications and Sensing. Norwood: MA: Artech House, 1999.
[4] A. D. Kersey, "Multiplexing techniques for fiber-optic sensors," in Optical Fiber Sensors: Applications, Analysis, and Future Trends, J. Dakin and B. Culshaw, Eds. Norwood: Artech House, 1997, pp. 373–376.
[5] M. G. Xu, H. Geiger, J. P. Dakin, Journal of Lightwave Technology **14**, 391 (1996).
[6] Y. J. Rao, Measurement Science and Technology **8**, 355 (19970.
[7] C. C. Chan, W. Jin, M. S. Demokan, Optics and Laser Technology **31**, 3199 (1999).
[8] C. C. Chan, C. Z. Shi, W. Jin, D. N. Wang, IEEE Photonics Technology Letters **15**(8), 1126 (2003).
[9] M. T. Heath, Scientific Computing: An Introductory Survey, 2nd ed. New York: McGraw-Hill, 2005.
[10] F. Lewis, Optimal Estimation. New York: John Wiley & Sons, Inc., 1986.
[11] H. E. Rauch, F. Tung, C. T. Striebel, AIAA Journal **3**(8), 1445 (1965).

*Corresponding author: pg03677467@ntu.edu.sg